Journal Pre-proof

Topographic Analysis of Lateral versus Medial Femoral Condyle Donor Sites for Oblong MFC Lesions

Atsushi Urita, MD, PhD, Michael L. Redondo, MA, BS, David R. Christian, BS, Hailey P. Huddleston, BS, Nozomu Inoue, MD, PhD, Brian J. Cole, MD, MBA, Adam B. Yanke, MD, PhD

PII: S0749-8063(20)30600-9

DOI: https://doi.org/10.1016/j.arthro.2020.07.007

Reference: YJARS 57033

To appear in: *Arthroscopy: The Journal of Arthroscopic and Related Surgery*

Received Date: 9 December 2019

Revised Date: 29 June 2020

Accepted Date: 3 July 2020

Please cite this article as: Urita A, Redondo ML, Christian DR, Huddleston HP, Inoue N, Cole BJ, Yanke AB, Topographic Analysis of Lateral versus Medial Femoral Condyle Donor Sites for Oblong MFC Lesions, *Arthroscopy: The Journal of Arthroscopic and Related Surgery* (2020), doi: https://doi.org/10.1016/j.arthro.2020.07.007.

Topographic Analysis of Lateral versus Medial Femoral Condyle Donor Sites for Oblong MFC Lesions

TBD: Atsushi Urita*, MD, PhD; Michael L. Redondo*, MA,BS; David R Christian*, BS; Hailey P. Huddleston, BS*; Nozomu Inoue†, MD, PhD; Brian J. Cole*, MD, MBA; Adam B. Yanke*, MD, PhD

* Division of Sports Medicine, Department of Orthopedic Surgery, Rush University Medical Center, Chicago, Illinois, U.S.A.

† Orthopaedic Biomechanics laboratory, Rush University Medical Center, Chicago, Illinois, USA

Corresponding Author:
Adam Yanke, MD PhD
Adam.Yanke@rushortho.com
Rush University Medical Center
1611 W. Harrison St.
Chicago, IL 60612

Topographic Analysis of Lateral versus Medial Femoral Condyle Donor Sites for Oblong MFC Lesions.

Abstract

Purpose: The primary objective of this study was to analyze the topographic matching of oblong osteochondral allografts (OCAs) to treat large oval MFC lesions using computer simulation models. The secondary objective was to determine whether LFC grafts would have a similar surface matching when compared with MFC grafts in this setting.

Methods: Human femoral hemi-condyles (10 MFCs, 7 LFCs) underwent three-dimensional computed tomography (CT). Models were created from CT images and exported into point-cloud models. Donor-recipient matches with large condylar width mismatch were excluded. The remaining specimen were divided into three donor-recipient groups with two defect sizes (17×30mm and 20×30mm): 20 MFC donor (MFCd)–MFC recipient (MFCr), 27 ipsilateral LFC donor (LFCd)–MFCr, and 26 contralateral LFCd–MFCr. Grafts were optimally virtually aligned with the MFCr defect. Mismatch of the articular cartilage and subchondral bone surfaces between the graft and the defect and articular step-off were calculated.

Results: MFCd grafts resulted in articular cartilage surface mismatch and peripheral step- of less than 0.5mm for both defect sizes. The subchondral bone surface mismatch was significantly greater than the articular cartilage surface mismatch ($P<.01$) in both defect sizes). Conversely, the ipsilateral and contralateral LFCd grafts resulted in significantly greater articular cartilage surface mismatch and step-off for both defect sizes when compared to MFCd grafts ($P<.01$).

Conclusion: Oblong MFC allografts provide acceptable topographic matching for large oval MFC lesions when condylar width differences are minimized. However, concern exists in utilizing oblong LFC allografts for MFC defects, as this can result in increased peripheral step-off and surface mismatch.

Clinical Relevance: This data reinforces the ability to utilize oblong MFC OCA for treating oval cartilage lesions of the MFC when condylar width is considered. Although other studies have demonstrated LFCs can be utilized to treat circular defects on the MFC, this may not be true for oblong grafts.

Introduction

Osteochondral allograft (OCA) transplantation has become a common procedure to treat full thickness chondral and/or osteochondral lesions.[1–3] Over the last few decades, OCA transplantation has proven to successfully restore the articular cartilage surface and improve clinical outcomes.[2,4–6] The surgical procedure, typically, involves the use of press-fit circular allografts because of the relative ease in achieving transplant fixation without supplemental internal fixation. [1,7]

Historically, large oval condylar defects have been treated using multiple dowels where multiple circular grafts are used to fill the lesion. Using multiple circular grafts, however, has several inherent limitations, such as increasing the number of interfaces that need to incorporate and/or achieving poor coverage of the lesion. Oblong OCAs offer an alternative for larger osteochondral lesions, potentially eliminating the need for multiple plugs in this setting.[8] However, topographic analysis is needed to clarify whether oblong OCAs can provide adequate articular cartilage surface topography and osseous matching for the treatment of large oval femoral condyle lesions.[9,10]

Limited graft availability is a constant concern when using OCA transplantation, especially for medial femoral condyle (MFC) lesions and the donor condyle can be matched via laterality, condyle (medial or lateral), and width of the affected condyle.[1,11] The matching process and limited tissue availability leads to increased patient wait times and prolongs time with symptoms. Although previous studies reported that lateral femoral condyle (LFC) circular OCAs provided similar surface matching as MFCd OCAs for the treatment of MFC lesions, the topographic matching of oblong LFC grafts for large MFC lesions remains unclear.[11–13]

The primary objective of this study was to analyze the topographic matching of oblong osteochondral allografts (OCAs) to treat large oval MFC lesions using computer simulation models. The secondary objective was to determine whether LFC grafts would have a similar surface matching when compared with MFC grafts in this setting. The hypothesis of this study was that (1) oblong MFCd grafts would provide acceptable topographic matching with large MFC defects, and (2) oblong LFCd grafts would result in greater mismatch with large MFC lesions than MFCd grafts.

Methods

Specimen Preparation

Seventeen distal fresh frozen femoral hemi-condyles with intact articular cartilage surface (10 MFC (5 right and 5 left) and 7 LFC (3 right and 4 left)) were acquired from a donor tissue bank (AlloSource, Denver, CO). No two condyles came from same the donor. Donor age and sex is not available. All specimens were evaluated by single investigator (ABY). Condylar width was measured using a digital micrometer positioned 10 mm distal to the most superior aspect of the notch, which is the same method used by donor tissue suppliers. Specimens with large condylar mismatch (> 5 mm difference or if the graft condylar width was smaller than the defect condylar width) were excluded. Three groups were created with the remaining specimen based on virtual donor-recipient combinations so that the condylar width of the donor was greater than that of the recipient: 20 MFC donor (MFCd) – MFC recipient (MFCr), 27 ipsilateral LFC donor (LFCd) – MFCr, and 26 contralateral LFCd – MFCr (**Figure 1**).

3D CT Computer Model Creation of the Distal Femoral Articular Surfaces

Specimen were completely thawed and then underwent computed tomography (CT) (BrightSpeed, GE Healthcare, Wauwatosa, WI) imaging in the coronal, axial, and sagittal planes by use of 0.625-mm continuous slices (120 kV, 100 mA, 1.0-mmsecond duration, 20-cm field of view, 512 x 512 matrices). Three dimensional (3D) CT models of the articular cartilage and bone were then created and exported into point-cloud models using a 3D reconstruction software program (Mimics, Materialise Inc., Leuven, Belgium). A local coordinate system was set on the distal femoral hemi-condyle **(Figure 2A)**. Eigenvectors of the distal femoral hemi-condyle point-cloud data set were

calculated to determine the orientation of orthogonal principal axes (x-, y-, and z-axes) of the distal femoral hemi-condyle as previously described **(Figure 2B)**.[11] A custom-written program coded in Microsoft Visual C ++ 2005 with Microsoft Foundation Class programming environment (Microsoft Corp., Redmond, WA) was used to perform the definition, the coordinate system, and 3D model creation, and geometry matching.

3D CT Computer Model Creation of Distal Femoral Condyle Defect and Graft Models

Oblong graft and defect models were created in the MFC and LFC with two different size of the oval shape; 17 mm width × 30 mm length and 20 mm width × 30 mm length. The centroid of the oval shape was determined as the most distal point of the articular cartilage surface in each distal femoral hemi-condyles **(Figure 3A)**. Subchondral bone graft models were created on the same location as articular cartilage graft models. Once the oval shape of articular cartilage was projected to the subchondral bone surface, the point-cloud data within those area was defined as the dataset of the subchondral bone graft and defect models **(Figure 3B)**.

3D Articular Surface Matching of Defect - Graft Condyles

The articular cartilage surface of the defect model was compared with the graft model in each combination. Including all groups, a total of 73 donor-recipient combinations were simulated using the two defect sizes (17 x 30 mm and 20 x30 mm), resulting in 146 defect-donor comparative combinations being tested. All examinations were performed by single investigator (ABY). The graft model was virtually placed on

the defect model. Orientation of the graft model was automatically adjusted to match the most anterior and posterior points of the graft model with those of the defect model **(Figure 4A)**. Distance of each point cloud between the articular cartilage surface of the graft and defect models was calculated so that the articular cartilage surface of the graft model matched with that of the defect model **(Figure 4B)**. The shortest distance from the point in the defect model to the corresponding point in the graft model was measured as the mismatch, where a perfect congruent match would equal a least mismatch of 0.00 mm for given data points on the simulated articular surface.[11,14,15] A mean value of the mismatch was calculated for each combination. Simultaneously, distance of each point cloud at the periphery between the graft and the defect models was calculated as the step-off **(Figure 4B)**. The shortest distance of each point cloud between the subchondral bone surface of the graft and defect models was calculated as the mismatch of the subchondral bone **(Figure 4B)**. This was performed for all combinations of simulated graft models and recipient models.

Statistical analysis

The data was presented as mean ± standard deviation. The data was analyzed using Excel 2010 (Microsoft Corp, Redmond, Washington) and JMP® software (v12.0, SAS Institute, Cary, NC). Statistical analysis was performed utilizing unpaired t-test to compare the condylar width between the MFC and the LFC. Paired t-test was performed to compare condylar width mismatch between defect sizes and to compare condylar width mismatch between the articular cartilage and the subchondral bone surface. Analysis of variance (ANOVA) was performed to compare the difference of condylar width, the mismatch of the articular cartilage surface, the step-off, and the mismatch of

the subchondral bone surface among groups. If the analysis of variance result was significant, post hoc analysis was performed with a Tukey HSD (honest significant difference) test. We utilized a threshold of 1 mm of surface incongruity to determine whether a graft provided adequate matching. Although the literature is conflicting on this topic and the clinical outcomes associated with a proud or sunken graft remain unclear, this threshold was chosen based on prior biomechanics studies and the experience of the senior authors.[9,10] To ensure the study was adequately powered, a post hoc power analysis was performed in G*Power. Based on the cartilage surface topography matching results (when the mean of one group is 0.5 and the other two groups are 1 with a SD of 0.4), we had a power of 99%. For the paired t-test analysis, we were powered to detect 0.2 – 0.3 mm difference between two groups when the standard deviation was 0.3 – 0.4 mm. Significance was set at $P < .05$.

Result

Specimen demographics

The mean condylar width was 24.7 ± 1.3 mm and 28.4 ± 1.3 mm for the MFC and LFC, respectively. Mean LFC width was significantly greater than mean MFC width ($P < .01$). The mean difference in condylar width between the donor and the recipient were 1.5 ± 1.2 mm in the MFCd – MFCr group, 4.1 ± 1.5 mm in the ipsilateral LFCd – MFCr group, and 4.3 ± 1.2 mm in the contralateral LFCd – MFCr group. The ipsilateral LFCd – MFCr and contralateral LFCd – MFCr groups exhibited significantly different mean difference in condyle width when compared to the MFCd – MFCr ($P < .01$ in both groups).

The articular cartilage surface matching between the graft and defect models

The articular cartilage surface mismatch is shown in **Table 1**. In the MFCd – MFCr group, the mismatch of the articular cartilage surface in the absolute value was less than 1.00 mm for all donor-recipient pairs at both 17 x 30 mm and 20 x 30 mm defect sizes. There was no significant difference in the articular cartilage mismatch between sizes ($P = 0.22$). Ipsilateral LFCd grafts and contralateral LFCd grafts exhibited significantly greater articular cartilage surface mismatch than MFCd grafts for the 17 x 30 mm defect and in the 20 x 30 mm defect ($P < .01$ in both groups, **Figure 5**). However, there was no significant difference between ipsilateral LFCd – MFCr and contralateral LFCd – MFCr groups ($P = 0.96$ in 17 x 30 mm defect and $P = 0.98$ in 20 x 30 mm).

Histograms showed that the MFCd grafts exhibited an articular cartilage surface mismatch within ± 1.00 mm in all combinations (**Figure 6A and C**). Conversely, the ipsilateral and contralateral LFCd grafts exhibited sunken articular cartilage surfaces

with 15 of 27 ipsilateral LFCd combinations (55.6%) and 13 of 26 contralateral LFCd combinations (50.0%) displaying an articular cartilage surface mismatch within ± 1.00 mm for the 17 x 30 mm defect (**Figure 6B and C**). Additionally, 14 of 27 ipsilateral LFCd combinations (51.9 %) and 9 of 26 contralateral LFCd combinations (34.6 %) exhibited articular cartilage surface mismatch within ± 1.00 mm for the 20 x 30 mm defect (**Figure 6E and F**).

Step-off at the periphery of the graft surrounding the defect

Mean step-off at the periphery of the graft around the defect is shown in **Table 2**. MFCd grafts provided a mean step-off mm within ±1.0 mm in all directions for both defect sizes (**Figure 7A**). In both defect sizes, the ipsilateral and contralateral LFCd grafts had a mean step-off of more than ±1.0 mm. In the 17x30 defect model, ipsilateral and contralateral LFCd grafts had a mean step-off of -0.90 ± 0.14 mm and -0.93 ± 0.46 mm, respectively. Similarly, when using the 20x30 defect model, ipsilateral and contralateral LFCd grafts had a mean step-off of -0.98 ± 0.43 mm and -0.98 ± 0.41 mm. A significantly greater mean step-off was exhibited in the ipsilateral and contralateral LFCd grafts than MFCd grafts for both defect sizes ($P < .01$ in both LFCd groups). The Ipsilateral and contralateral LFCd allograft step-offs were significantly greater in the medial and lateral portions than that at the anterior and posterior portions (**Figure 7B and C**).

The subchondral bone surface matching between the graft and recipient models

The mean least distances of subchondral bone surface mismatch are shown in **Table 3**. In MFCd grafts, the mismatch of the subchondral bone surface was approximately

1.0 mm for both defect sizes, and exhibited a significant difference when compared with the articular cartilage surface mismatch (P < .01 in both defect sizes). In ipsilateral LFCd allografts, the subchondral bone surface mismatch was greater than the MFCd allografts (P < .01 in both defect sizes). While contralateral LFCd grafts exhibited significantly greater mismatch of the subchondral bone surface than MFCd grafts in 17x30 mm defect (P < .01), no significant difference of subchondral bone surface mismatch was found in the 20 x 30 mm defect between MFCd and contralateral LFCd grafts (P = 0.608).

Discussion

The main finding of this study was that MFCd oblong grafts provided adequate surface topography matching and peripheral step-off (< 1 mm) and were superior to ipsilateral and contralateral LFCd grafts. Furthermore, ipsilateral and contralateral LFCd allografts provided 1.0 mm or more mean mismatch of the articular cartilage surface. Furthermore, the mean step-off of the ipsilateral LFCd and contralateral LFCd grafts were greater. These findings suggest that an LFCd oblong graft may not be an adequate substitute for an MFCd oblong graft when treating an MFC chondral defect.

Due to the average anatomic width (<25mm) of the MFC, larger defects typically extend in an ovoid fashion, and can no longer be estimated by true circles. In this study, the mean MFC condylar width was 24.7 ± 1.3 mm, and two longitudinal lesion sizes (17 x 30 mm; 20 x 30 mm) were investigated. The condylar width of LFCds (28.4 ± 1.3 mm) was found to be significantly greater than that of the MFCrs (24.7 ± 1.3 mm). Additionally, the mean difference in condylar width of both LFCd – MFCr groups (ipsilateral LCFd – MFCr: 4.1 ± 1.5 mm; contralateral LFCd – MFCr: 4.3 ± 1.2 mm)

were found to be greater than that of the MFCd – MFCr group. Together, the information suggests that oblong LFCd grafts would be able to provide ample coverage of large MFC lesions.

Previous studies have shown the surface matching of circular OCAs for distal femoral condyle defects.[11–13] Mologne et al. investigated the articular cartilage surface match of OCAs for the treatment of circular MFC defects.[13] The authors showed that MFCd grafts yielded a mean articular cartilage surface mismatch of 0.64 mm and a mean step off of 0.45 mm. Berstein et al examined matching the radius of OCAs curvature with the recipient condyles in 3 zones of the femoral condyle.[12] They reported a mean mismatch of -0.09 mm with a mean maximum protrusion of 0.59 mm and a mean maximum recession of -0.74mm. Furthermore, Yanke et al. used topographic analysis to examine the mismatch of circular, femoral condyle OCAs to treat focal condylar cartilage defects.[11] The authors demonstrated that the OCAs used to treat defects from the same condyle yielded a mismatch of 0.45 to 0.62 mm and utilizing circular OCAs can offer precise surface matching for MFC cartilage lesions. In the current study, the articular cartilage surface matching of oblong MFCd grafts was consistent with the previous topographic analysis of circular OCAs, suggesting that MFCd grafts may be a potential source of oblong OCAs for treating large longitudinal MFC lesions.

The OCA step-off at the defect periphery has been shown to impact the biomechanical properties of the transplantation.[9,16–18] D'Lima et al. showed that grafts proud by 0.5 mm increase peak contact stress up to two times the contact pressure of intact native cartilage.[16] Koh et al. demonstrated plugs elevated 1.0 and 0.5 mm above the surrounding surface had significantly increased peak contact pressure, and that plugs

sunk 0.5 and 1.0 mm below the surrounding surface significantly increased the peak contact pressure upon the surrounding intact area.[9] In this study, the mean step-off of oblong MFCd grafts was less than 0.50 mm for the 17 x 30 mm and 20 x 30 mm MFCr lesions. These results suggest that the oblong MFCd grafts may provide acceptable biomechanical properties for MFC longitudinal defects.

As graft availability is a major concern of OCA transplantation and can lead to significant delay due to donor availably, it is important to understand if LFC grafts can produce similar surface topography matching to MFC grafts for treatment of MFC defects. While many surgeons prefer to treat MFC defects with MFCd allografts, prior in vitro studies have suggested that LFC grafts for an MFC defect may provide acceptable results.[19,20] For example, an investigation by Molonge et al. demonstrated that circular LFCd grafts provided comparable and favorable topographic matching when compared to MFCd grafts.[13] The clinical ramifications of these in vitro finding remains unclear. A clinical study by Wang et al. compared outcomes in two groups: one group that received orthotopic (LFC graft for LFC defect or MFC graft for MFC defect) grafts and one that received non-orthotropic grafts (LFC graft for MFC defect or MFC graft for LFC defect). They found that there were no significant differences in patient reported outcomes between the two cohorts. While our study found that LFCd grafts provide inferior surface topography matching compared to MFCd grafts for treating large MFC defects (only about 50% of grafts provided clinically acceptable surface topography mismatch), future studies are needed to evaluate the clinical correlates of these findings.

Limitations

There are several limitations in this study. First, the simulated defect was created in a single location and alternative defect locations were not investigated. Articular cartilage lesions can be located at the various areas in the MFC. At other defect locations, mismatch may be greater than in central lesions and our study does not investigate or account for this. Second, differences of biomechanical properties between OCAs and recipients were not investigated. Biomechanical properties of oblong OCAs may be inferior to circular OCAs because of the stability of the graft for the recipient. These variables have not been explored in this study and warrant future analysis. In addition, the degree of mismatch was not compared to treating the same defect with multiple circular OCAs, a commonly used technique for large longitudinal MFC lesions.[8] Future studies should investigate the differences in surface incongruity between these two approaches.

Conclusion

Oblong MFC allografts provide acceptable topographic matching for large oval MFC lesions when condylar width differences are minimized. However, concern exists in utilizing oblong LFC allografts for MFC defects, as this can result in increased peripheral step-off and surface mismatch.

References**:**

1. Cole BJ, Pascual-Garrido C, Grumet RC. Surgical management of articular cartilage defects in the knee. *J Bone Jt Surg Am Volume*. 2009;91(7):1778-1790.

2. Frank RM, Lee S, Levy D, et al. Osteochondral Allograft Transplantation of the Knee: Analysis of Failures at 5 Years. *Am J Sports Medicine*. 2017;45(4):864-874. doi:10.1177/0363546516676072

3. Levy Y, Görtz S, Pulido P, McCauley J, Bugbee W. Do Fresh Osteochondral Allografts Successfully Treat Femoral Condyle Lesions? *Clin Orthop Relat R*. 2013;471(1):231-237. doi:10.1007/s11999-012-2556-4

4. Cameron JI, Pulido PA, McCauley JC, Bugbee WD. Osteochondral Allograft Transplantation of the Femoral Trochlea. *Am J Sports Medicine*. 2016;44(3):633-638. doi:10.1177/0363546515620193

5. Krych AJ, Pareek A, King AH, Johnson NR, Stuart MJ, Williams RJ. Return to sport after the surgical management of articular cartilage lesions in the knee: a meta-analysis. *Knee Surg Sports Traumatology Arthrosc*. 2017;25(10):3186-3196. doi:10.1007/s00167-016-4262-3

6. Shaha J, Cook J, Rowles D, Bottoni C, Shaha S, Tokish J. Return to an athletic lifestyle after osteochondral allograft transplantation of the knee. *Am J Sports Medicine*. 2013;41(9):2083-2089. doi:10.1177/0363546513494355

7. Hennig A, Abate J. Osteochondral Allografts in the Treatment of Articular Cartilage Injuries of the Knee. *Sports Med Arthrosc*. 2007;15(3):126-132. doi:10.1097/jsa.0b013e31812e5373

8. Godin JA, Sanchez G, Cinque ME, Chahla J, Kennedy NI, Provencher MT. Osteochondral Allograft Transplantation for Treatment of Medial Femoral Condyle Defect. *Arthrosc Techniques*. 2017;6(4):e1239-e1244. doi:10.1016/j.eats.2017.04.010

9. Koh J, Wirsing K, Lautenschlager E, Zhang L. The effect of graft height mismatch on contact pressure following osteochondral grafting: a biomechanical study. *Am J Sports Medicine*. 2004;32(2):317-320. doi:10.1177/0363546503261730

10. Du PZ, Markolf KL, Boguszewski DV, et al. Effects of Proud Large Osteochondral Plugs on Contact Forces and Knee Kinematics: A Robotic Study. *Am J Sports Medicine*. 2018;46(9):2122-2127. doi:10.1177/0363546518770415

11. Yanke A, Urita A, Shin J, et al. Topographic Analysis of the Distal Femoral Condyle Articular Cartilage Surface: Adequacy of the Graft from Opposite Condyles of the Same or Different Size for the Osteochondral Allograft Transplantation. *Cartilage*. 2018;10(2):205-213. doi:10.1177/1947603517752056

12. Bernstein D, O'Neill C, Kim R, et al. Osteochondral Allograft Donor-Host Matching by the Femoral Condyle Radius of Curvature. *Am J Sports Medicine*. 2016;45(2):403-409. doi:10.1177/0363546516671519

13. Mologne TS, Cory E, Hansen BC, et al. Osteochondral allograft transplant to the medial femoral condyle using a medial or lateral femoral condyle allograft: is there a difference in graft sources? *Am J Sports Medicine*. 2014;42(9):2205-2213. doi:10.1177/0363546514540446

14. Gupta AK, Forsythe B, Lee AS, et al. Topographic analysis of the glenoid and proximal medial tibial articular surfaces: a search for the ideal match for glenoid resurfacing. *Am J Sports Medicine*. 2013;41(8):1893-1899. doi:10.1177/0363546513484126

15. Shin JJ, Haro M, Yanke AB, et al. Topographic analysis of the capitellum and distal femoral condyle: finding the best match for treating osteochondral defects of the humeral capitellum. *Arthrosc J Arthrosc Relat Surg Official Publ Arthrosc Assoc North Am Int Arthrosc Assoc*. 2015;31(5):843-849. doi:10.1016/j.arthro.2014.11.039

16. D'Lima DD, Chen PC, Colwell CW. Osteochondral grafting: effect of graft alignment, material properties, and articular geometry. *Open Orthop J*. 2009;3(1):61-68. doi:10.2174/1874325000903010061

17. Koh J, Kowalski A, Lautenschlager E. The effect of angled osteochondral grafting on contact pressure: a biomechanical study. *Am J Sports Medicine*. 2005;34(1):116-119. doi:10.1177/0363546505281236

18. Nakagawa Y, Suzuki T, Kuroki H, Kobayashi M, Okamoto Y, Nakamura T. The effect of surface incongruity of grafted plugs in osteochondral grafting: a report of five cases. *Knee Surg Sports Traumatology Arthrosc*. 2007;15(5):591-596. doi:10.1007/s00167-006-0253-0

19. Duan C, Orías A, Shott S, et al. In vivo measurement of the subchondral bone thickness of lumbar facet joint using magnetic resonance imaging. *Osteoarthr Cartilage*. 2011;19(1):96-102. doi:10.1016/j.joca.2010.10.015

20. Li G, Park S, DeFrate L, et al. The cartilage thickness distribution in the tibiofemoral joint and its correlation with cartilage-to-cartilage contact. *Clin Biomechanics Bristol Avon*. 2005;20(7):736-744. doi:10.1016/j.clinbiomech.2005.04.001

Figure 1. Diagram of donor – recipient groups. Medial femoral condyle donor (MFCd) – MFC recipient (MFCr), Ipsilateral lateral femoral condyle donor (LFCd) – MFCr, and Contralateral LFCd – MFCr were created based on the difference between the donor and the recipient condylar width.

Figure 2. (A) An orthogonal local coordinate system (x-, y- z-axes) of the femoral hemi-condyle was set with the orientation determined by the intersection (yellow dot) of three planes (blue, red, and green planes). The most distal (along the z-axis) point was determined (cyan blue dot). (B) The en face of projection of the femoral hemi-condyle surface was used for point-cloud data analysis.

Figure 3. Three-dimensional defect and graft model creation of distal femoral condyle. (A) Oblong defect models were created in the medial femoral condyle (MFC) and graft models in the MFC and the lateral femoral condyle (LFC). The ceontroid of the oval shape was determined as the most distal point of the articular cartilage surface (cyan blue dot). (B) The subchondral bone defect and graft models were created by the projection of the articular cartilage models.

Figure 4. Three-dimensional surface geometries of the articular surface and subchondral bone surface were compared between the defect and the graft models. (A) The defect model was virtually placed on the surface of the graft model. Eigenvectors of the graft and the defect models were oriented to each other until they matched. (B) mismatch of articular surface and resulting subchondral bone surface and step-off at the periphery of the graft were calculated.

Figure 5. A 3-dimensional representation of the distance distribution of the articular cartilage surface of the 20 x 30 mm graft model superimposed on the left medial femoral condyle. The blue gradient color represents penetration into the defect model, whereas red represents prominence. The white color indicates perfect congruence between the defect and the graft models.

Figure 6. Histogram of articular cartilage surface mismatch deviation from defect models for medial for medial femoral condyle donor (A), ipsilateral lateral femoral condyle (LFC) donor (B), and contralateral LFC donor (C).

Figure 7. Polar plots of step-off height for representative medial femoral condyle donor (A), ipsilateral lateral femoral condyle (LFC) donor (B), and contralateral LFC donor (C).

Figure 8. A 3-dimensional representation of the distance distribution of the resulting subchondral bone surface of the 20 x 30 mm graft model superimposed on the left medial femoral condyle. The blue gradient color represents penetration into the defect model, whereas red represents prominence. The white color indicates perfect congruence between the defect and the graft models.

Table 1. The Mean Least Distance of the Articular Cartilage Surface

Defect Size, mm	MFC	Donor Condyle, mm Ipsi-LFC	Cont-LFCd	ANOVA*	MFC vs Ipsi-LFC	MFC vs Cont-LFC:	Ipsi-LFC vs Cont-LFC
17 x 30	0.5 ± 0. 2	1.0 ± 0.3	1.0 ± 0.4	*P* < .01	*P* < .01	*P* = 0.56	*P* = 0.20
20 x 30	0.5 ± 0.1	1.1 ± 0.4	1.1 ± 0.4	*P* < .01	*P* <.01	*P* <.01	*P* = 0.98

NOTE. Data presented as mean ± standard deviation.
*Statistical comparison of the mean least distance among donor condyles.
MFC, medial distal femoral condyle; LFC, lateral distal femoral condyle; Ipsi, ipsilateral; Cont, contralateral.

Table 2. Step-off at the Periphery of the Defect

Defect Size (mm)	MFC	Donor Condyle, mm Ipsi-LFC	Cont-LFC	ANOVA*	MFC vs Ipsi-LFC	MFC vs Cont-LFC:	Ipsi-LFC vs Cont-LFC
17x30	-0.3 ± 1.0	-0.9 ± 0.1	-0.9 ± 0.5	*P* < .01	*P* <.01	*P* <.01	*P* = 0.80
20x30	-0.10 ± 0.45	-1.0 ± 0.4	-1.0 ± 0.4	*P* < .01	*P* <.01	*P* <.01	*P* = 0.95

NOTE. Data presented as mean ± standard deviation.
*Statistical comparison of the step-off at the periphery of the defect among donor condyles.
MFC, medial distal femoral condyle; LFC, lateral distal femoral condyle; Ipsi, ipsilateral; Cont, contralateral.

Table 3. The Mean Least Distance of the Subchondral Bone Surface

Defect Size, mm	MFC	Donor Condyle, mm Ipsi-LFC	Cont-LFC	ANOVA*	MFC vs Ipsi-LFC	MFC vs Cont-LFC:	Ipsi-LFC vs Cont-LFC
17 x 30	1.0 ± 0.4	1.4 ± 0.8	1.2 ± 0.4	*P* <.01	*P* <.01	*P* <.01	*P* = 0.96
20 x 30	1.0 ± 0.4	1.7 ± 1.0	1.2 ± 0.3	*P* < .01	*P* < .01	*P* = 0.61	*P* = 0.03

NOTE. Data presented as mean ± standard deviation.
*Statistical comparison of the mean least distance among donor condyles.
MFC, medial distal femoral condyle; LFC, lateral distal femoral condyle; Ipsi, ipsilateral; Cont, contralateral.

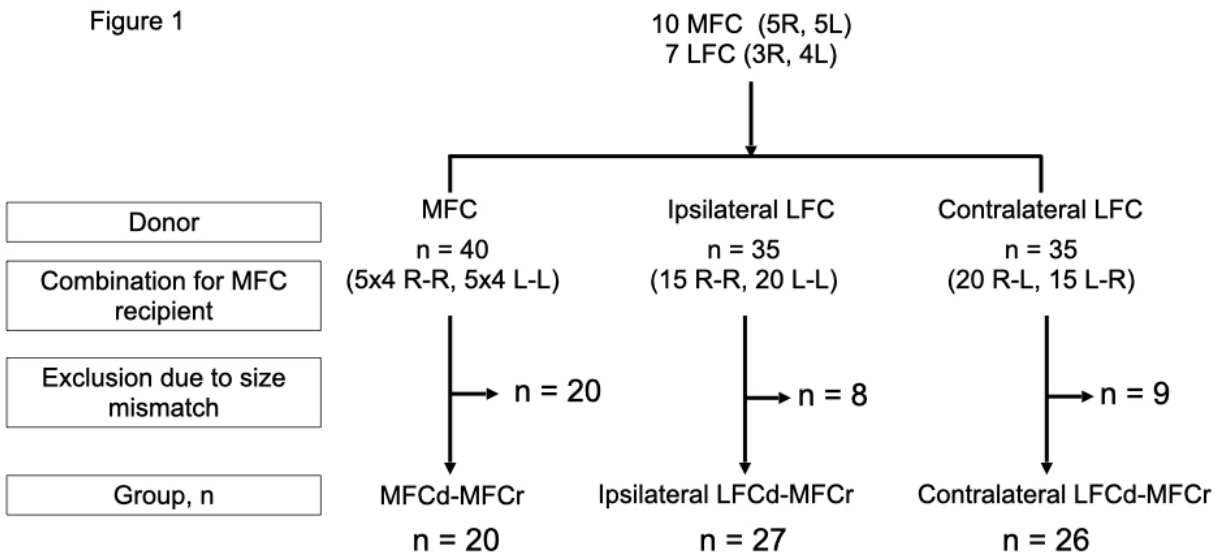

Figure 1. Diagram of donor – recipient groups. Medial femoral condyle donor (MFCd) – MFC recipient (MFCr), Ipsilateral lateral femoral condyle donor (LFCd) – MFCr, and Contralateral LFCd – MFCr were created based on the difference between the donor and the recipient condylar width.

Figure 2

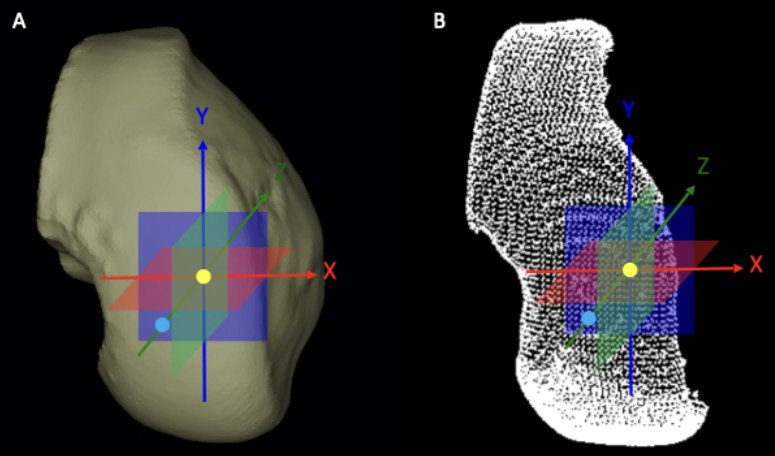

(A) An orthogonal local coordinate system (x-, y- z-axes) of the femoral hemi-condyle was set with the orientation determined by the intersection (yellow dot) of three planes (blue, red, and green planes). The most distal (along the z-axis) point was determined (cyan blue dot). (B) The en face of projection of the femoral hemi-condyle surface was used for point-cloud data analysis.

Figure 3

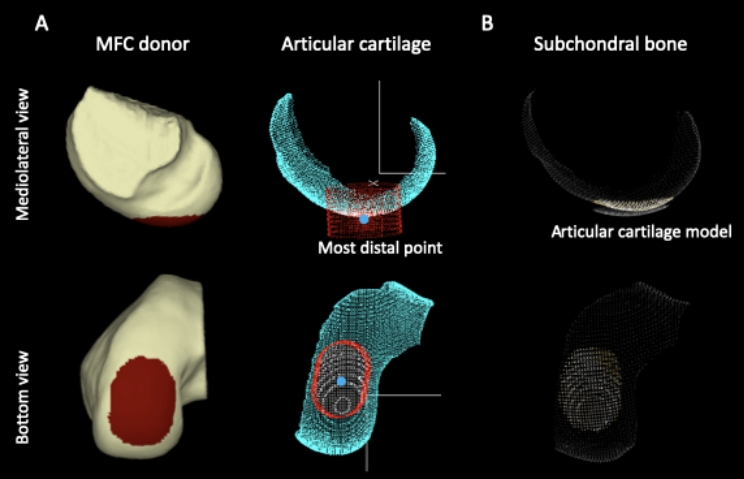

(A) Oblong defect models were created in the medial femoral condyle (MFC) and graft models in the MFC and the lateral femoral condyle (LFC). The ceontroid of the oval shape was determined as the most distal point of the articular cartilage surface (cyan blue dot). (B) The subchondral bone defect and graft models were created by the projection of the articular cartilage models.

Figure 4

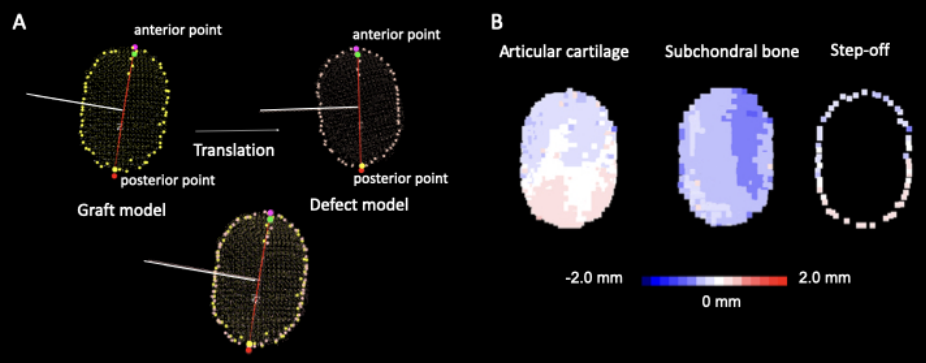

Three-dimensional surface geometries of the articular surface and subchondral bone surface were compared between the defect and the graft models. (A) The defect model was virtually placed on the surface of the graft model. Eigenvectors of the graft and the defect models were oriented to each other until they matched. (B) mismatch of articular surface and resulting subchondral bone surface and step-off at the periphery of the graft were calculated.

Figure 5

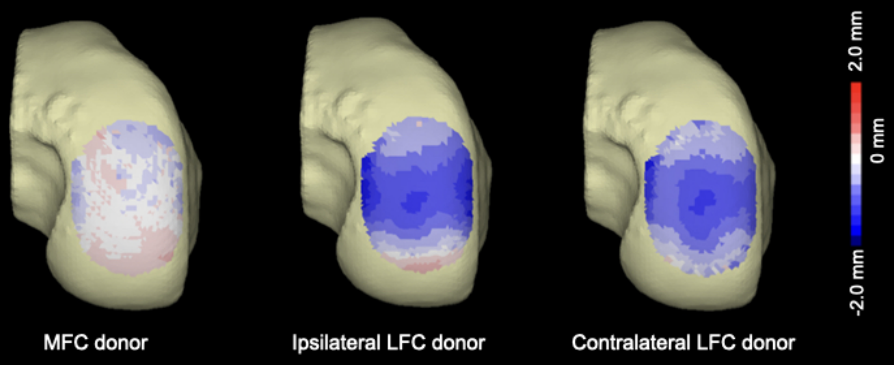

A 3-dimensional representation of the distance distribution of the articular cartilage surface of the 20 x 30 mm graft model superimposed on the left medial femoral condyle. The blue gradient color represents penetration into the defect model, whereas red represents prominence. The white color indicates perfect congruence between the defect and the graft models.

Figure 6

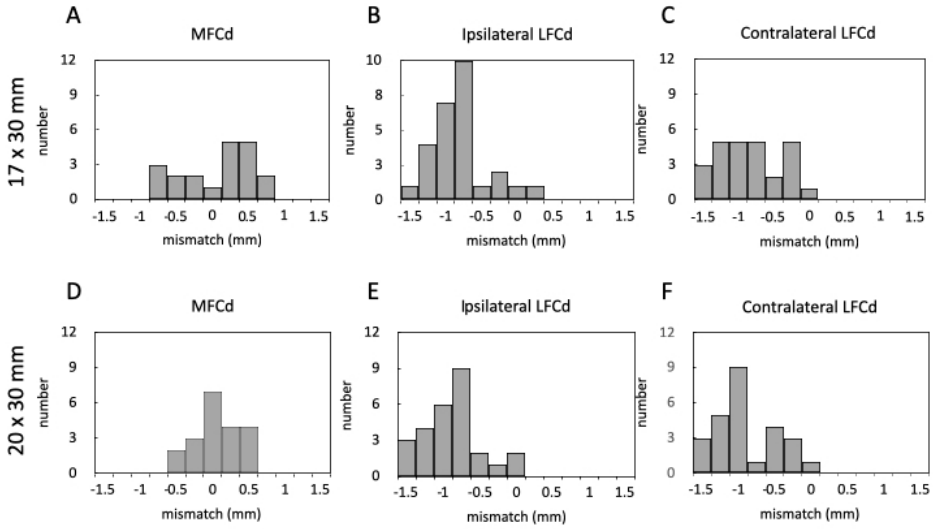

Histogram of mismatch deviation from defect models for medial for medial femoral condyle donor (A), ipsilateral lateral femoral condyle (LFC) donor (B), and contralateral LFC donor (C).

Figure 7

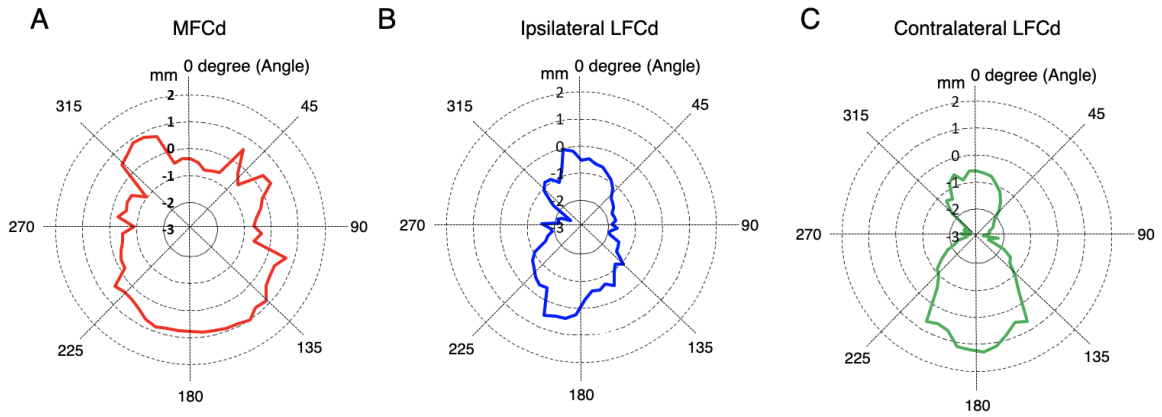

Polar plots of step-off height for representative medial femoral condyle donor (A), ipsilateral lateral femoral condyle (LFC) donor (B), and contralateral LFC donor (C).

Figure 8

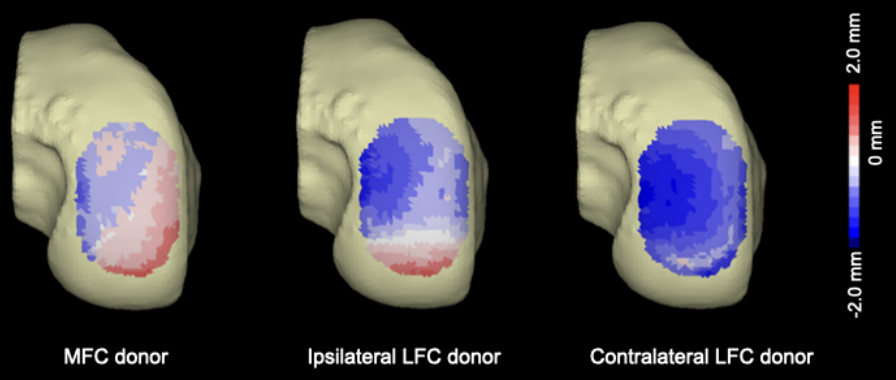

A 3-dimensional representation of the distance distribution of the resulting subchondral bone surface of the 20 x 30 mm graft model superimposed on the left medial femoral condyle. The blue gradient color represents penetration into the defect model, whereas red represents prominence. The white color indicates perfect congruence between the defect and the graft models.